Proceedings of the 8th European Conference of the Prognostics and Health Management Society 2024 - ISBN – 978-1-936263-40-0

On the Feasibility of Condition Monitoring of Belt Splices in Belt Conveyor Systems Using IoT Devices*

Henrik Lindström[1], Johan Öhman[2], Vanessa Meulenberg[3], Reiner Gnauert[4], Claus Weimann[5], and Wolfgang Birk[6]

[1,2,3,6] Predge AB, Västra Varvsgatan 11, 97234 Luleå, Sweden
{Henrik.Lindstrom,Johan.Ohman ,Vanessa.Meulenberg, Wolfgang.Birk}@predge.se

[6] Automatic Control, Luleå University of Technology, 97187 Luleå, Sweden
Wolfgang.Birk@ltu.se

[4,5] HOSCH Fördertechnik GmbH, Am Stadion 36, 45659 Recklinghausen, Germany
{Reiner.Gnauert, Claus.Weimann}@hosch.de

Abstract

This paper investigates fully automated condition monitoring of belt splices within operational belt conveyor systems, using IoT devices to predict and inform on potential belt breakage or tearing. Such events cause production stops and potentially harm workers. Belt splices are laminated belt connections subject to deterioration during operation and are usually weak spots. The proposed scheme circumvents manual inspection efforts and uses the HOSCH[iris] DISCOVER IoT device for sensing and data acquisition. Each belt conveyor is equipped with one individual IoT device acquiring the motion signal of the scraper which is used to learn signal patterns of the pulley and the belt to identify both location and deterioration of the individual splices. Deterioration is characterized from an initial healthy condition to a severe condition of the splice to inform on the potential need for action. To assess the feasibility of the scheme, several tests are designed and performed in an industrial belt conveyor system. The results indicate that the scheme can provide valuable insights into the splice condition and its degradation.

1. Introduction

Belt conveyor systems are widely used to transport material and are an essential component in many industry sectors but are often critical assets in a production chain of bulk material, like in e.g. mining. Unexpected breakdowns of belt conveyor systems render production stops, losses, and can severely harm workers in close perimeter of such events.

The belt usually consists of several pieces, vulcanized together to achieve sufficient length. The vulcanized joints are called splices. In Figure 1, a simplified sketch of a belt conveyor is shown, and how splices could be distributed along the belt. The condition of these splices deteriorates during operation, leading to breakage or tearing. To preventively detect damage, all splices are regularly inspected. For this, the belt is run empty and at low speed to visually assess the belt surface and splices by a worker, leading to frequent downtimes in production. The quality of this manual condition assessment depends on the workers' expertise to identify issues on a moving belt, while keeping sufficiently attentive and tracking the splice locations. Such a campaign can last for several hours for longer belt conveyors, and thus human errors are not uncommon. To circumvent the problem of production losses, there is a need for monitoring solutions that work during normal operation.

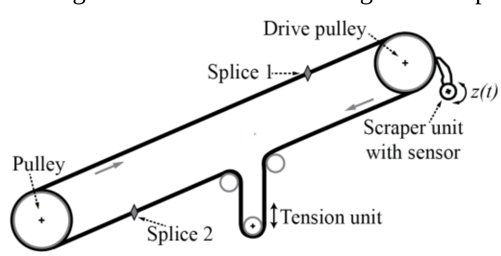

Figure 1: Sketch of the belt conveyor system with two splices and a scraper unit equipped with the sensing device generating the output $\boldsymbol{z(t)}$.

Various methods have been proposed for monitoring steel cord belt splices. Min (2010) suggests using Hall effect sensors to measure belt deformation and bending moment equations to assess the tensile force. However, concrete results validating this technique are lacking. Harrison (1985) and Kozłowski et al. (2020) propose methods based on measuring magnetic fields generated by belt reinforcement steel cords. Kozłowski, et.al. (2020) found that through a variability analysis, the magnetic current can be compared to an estimated pattern. With this method, the cords could be monitored. Bancroft et al. (2017) used a camera and encoder to visually inspect mechanical splices and could determine the splice condition. Alport et al. (2001) developed artificial neural networks for splice monitoring using conveyor belt video footage, achieving splice identification accuracy of at least 89%. However, further development is needed for monitoring splice degradation and internal defects. Roxon Oy's HX products utilize laser scanning for surface damage and for monitoring the belt thickness that could detect splice elongation (Roxon, 2024).

The solutions discussed above require splices with steel cord reinforcement or mechanical splices that are easily visible. A camera installation or laser scanner, even though it has potential, requires the additional installation of equipment, resulting in increased maintenance costs. Moreover, the methods described above frequently lack definitive results regarding their accuracy.

The contribution of this paper is an analytics solution for condition monitoring of belt splices utilizing the displacement data from one individual belt scraper, as patented by Weimann and Kiel (2020). The benefit of this approach is that it can be used for all belt configurations, while in operation and with material on the belt. Since only the displacement of the scraper is analyzed, no additional equipment is required, making it a cost-effective solution.

The paper is structured as follows. First, a problem definition and description of the approach is given, followed by a summary of the scraper sensing solution. Next, the analytics solution is described, including belt speed estimation, transformation to distance domain, belt signature estimation, splice re-identification and degradation, and condition estimation. Thereafter, the proposed method is applied and tested in a real-life setting and the results are presented and discussed. Finally, the work is concluded.

2. Problem Definition and Approach

Splices are fixed locations on a belt which means that the individual splice locations need to be re-identified in $z(t)$, which is the displacement of the scraper (Figure 1). While $z(t)$ is time-based, the splice itself has a spatial location and structure along the belt. The problem of the condition monitoring of a splice over time is therefore to identify the passage of an individual splice at the sensor and to assess its degradation based on the signal that is acquired during the passage of the splice at the sensor. Moreover, the belt speed is not constant and needs to be treated as unknown. Using an individual IoT device combined with the scraper to measure $z(t)$ would avoid any integration of the sensing solution with the control system or IT infrastructure, making deployment easy and fast.

The approach to address the problem is as follows: The HOSCH[iris] DISCOVER System is selected as the IoT device measuring the displacement $z(t)$ of the scraper. From the measurement and using design information of the pulley, the belt speed is estimated. Thereafter, the measurement signal $z(t)$ is transformed into the spatial or distance domain, denoted $z(d)$, where d denotes the distance that is covered. The annotated locations of the splices in the distance domain can then be re-identified in $z(d)$ requiring the detection of complete belt revolutions in the data. For every revolution of the belt, the splice locations can then be assessed, and their change can be tracked over the number of belt revolutions or time. Using the change in $z(d_i)$ for splice i at location d_i, condition indicators are derived and then mapped into actionable insights for decision making on maintenance or stopping of the belt conveyor.

Some challenges to this approach must be addressed. First, the measurement signal is affected by noise, which come from the surface structure of the belt and the pulley, but also from the scraping action to remove material from the belt. It is also not uncommon that material can get stuck between the scraper and the belt for some time which can lead to a temporary large displacement signal. How these effects will be managed is described in Section 4.

Moreover, the solution is intended to work independently of a control system or any integration into the IT infrastructure of the belt conveyor owners. The solution is therefore implemented in a cloud-based architecture as depicted in Figure 2. There, the IoT device connects with the HOSCH cloud to ingest the data and makes it accessible for the analytics in the partnering Predge cloud. All front-end functionalities are collected in HOSCH cloud, like configuration, alarming, visualization of actionable insights on the splices, and dashboards for the decision making of the user.

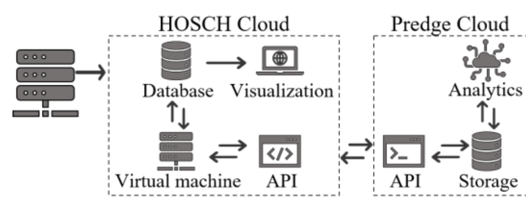

Figure 2: Cloud architecture to acquire the IoT device data, store and process it to provide actionable insights.

3. Sensing Solution

In this section, a short description is given of the sensing solution, based on the patent by Weimann et al. (2020). Figure 3 depicts a sketch of the scraper at the drive pulley on the belt, including the sensor. The pulley has a lining generating a high friction surface that is in contact with the belt. In the current setup, the high friction surface consists of three segments. The scraper is fixed to an axle where it can rotate. Connected to the scraper is a spring rod to adjust the tension at which the scraper is in contact with the belt. The spring rod will move proportionally to the scraper. Opposite the spring rod, there is a sensor mounted to the housing which measures the distance between the sensor and a magnet attached to the end of the spring rod.

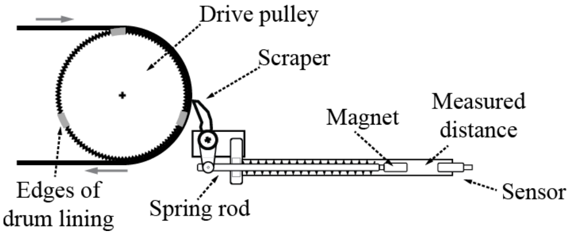

Figure 3. HOSCH HD PU pre scraper connected to the pre-tensioning spring and sensing device.

In **Error! Reference source not found.**, the raw sensor s ignal is displayed showing approximately 16 meters of the belt passing by the sensor, where the speed was increased at 12:22:07. The recurrent sinusoidal-like motion originates from the surface structure of the pulley where the drum is equipped with a lining composed of several segments. It is important to note that the pulley surface is a disturbance in the signal and may mask the belt surface changes. When the speed is increased the pulley rotational speed is increasing which leads to an increase in the frequency of the sinusoidal-like disturbance.

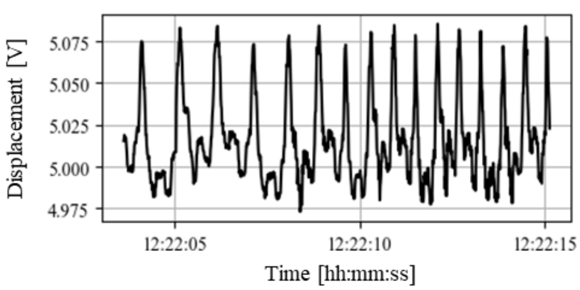

Figure 4. Raw sensor signal for a short time where the conveyor belt is run at two different speeds.

The sensor is connected to the IoT measurement system that samples the sensor signal and pre-processes it. It is thereafter locally stored and transmitted to the cloud wirelessly.

4. Analytics Solution

In this section the analytics solution to determine the condition of splices on a belt is presented.

4.1. Overview

The condition monitoring of splices using the scraper displacement measurement $z(t)$ requires several steps, as shown in Figure 5. One reason for this is that the splices are not as prominent in the sensor signal as the joined effect of all disturbances, like sensor noise, surface structures of pulley and belt, and displacement due to material removal from the belt. Consequently, the algorithm needs to recover the displacement that is attributed to the splices. In addition, the displacement needs to be correctly assigned to an individual splice to assess the surface change at the splice location.

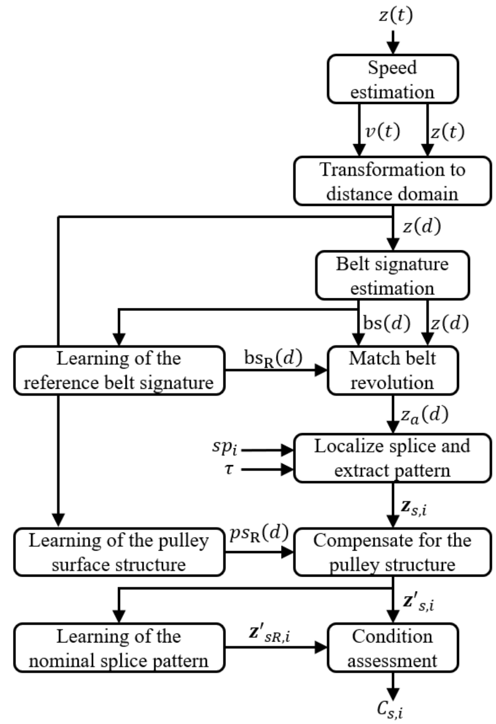

Figure 5. Block diagram for the condition monitoring of splices.

To ensure that surface changes are correctly assigned, the measured displacements need to be associated with specific locations along the belt. By estimating the belt speed from the measurement signal, transforming it into the distance domain and then identifying complete revolutions of the belt, it is possible to associate displacement measurements with specific coordinates along the belt. The identification of complete revolutions is done using an estimate for the belt surface signature, denoted $bs(d)$.

After an initial learning of a reference belt signature $bs_R(d)$, it is possible to match a complete revolution. Since splices are fixed locations sp_i along the belt with an overestimated length τ, a distance series can be extracted from the aligned raw data $z_a(d)$, reflecting the splice location, denoted $\boldsymbol{z}_{s,i}$. Since the pulley rotation and belt rotations are not aligned, the displacement induced by the pulley surface structure needs to be compensated for rendering $\boldsymbol{z}'_{s,i}$. Now the change in the surface can either be assessed in absolute terms or relative to a nominal $\boldsymbol{z}'_{sR,i}$, which is learned from data or provided by the user. The surface change can be assessed in different way and renders a condition indicator $C_{s,i}$. An advantage of this approach is that local belt damages are not confusing the association of splices to specific data series which enables the detection of new monitoring locations.

4.2. Speed estimation

To analyse the splice condition, the belt speed $v(t)$, needs to be estimated. The edges of the lining segments on the pulley introduce a distorted sinusoidal structure to the displacement data $z(t)$. This reoccurring structure in the signal is utilized when estimating the speed of the belt, by measuring the time between two registered edges and converting the time to a velocity. The displacement data $z(t)$ is split into five second batches of data $X(t)$, such that small changes in speed can be registered. $X(t)$ is now assumed to be a stationary process and can be normalized as

$$X' = \frac{X - \bar{X}}{\sigma} \tag{1}$$

where $\bar{X}$ is the mean and σ is the standard deviation of X. The normalization in (1) is done such that when computing the autocorrelation function (ACF) of the batch, there will not be any variance offset present. The ACF for a stationary process is defined as

$$r_{X'}(\tau) = \int_{-\infty}^{\infty} X'(t)X'(t+\tau)\mathrm{dt}. \tag{2}$$

The ACF in (2) is used here because of the repetitiveness of $z(t)$. The ACF will show local maxima at distances away from zero corresponding to the time it takes for the next lining segment to appear. Let i' be the solution to the following minimization problem that searches for the index in $r_{X'}(\tau)$ that corresponds to the first local maxima.

$$\begin{aligned} \text{Minimize} \quad & i \in \mathrm{dom}(r_{X'}) \\ \text{s. t.} \quad & i \geq m \\ & r_{X'}(i) \geq h \\ & \nabla r_{X'}(i) = 0 \\ & \Delta r_{X'}(i) < 0 \end{aligned} \tag{3}$$

In (3), m is a lower limit of i, h is a lower limit of $r_{X'}$ at index i and the third and fourth criterions requires i to be at a local maximum to $r_{X'}$. The solution i' to (3) is then the smallest index which satisfies all the criterions for (3). The velocity of the belt is calculated as

$$v = \frac{D}{3i'} \tag{4}$$

where D is the circumference of the pulley. The calculations in (2), (3) and (4) are done for each batch, resulting in a vector of speed estimations that will later be used for transforming the time series into a distance series.

4.3. Transformation to distance domain

If the average speed in the speed vector was greater than 0.2 m/s, $z(t)$ is transformed into a distance series, $z(d)$. The time series signal is sampled at a fixed rate at instance k independent of the belt speed. The covered distance d_k by the belt is a multiplication of the time instances t_k by the belt speed $v(t_k)$. The resulting distance dependent series $z(d_k)$ is not sampled equidistantly. By applying a linear interpolation with a fixed distance sample rate of 1 cm, an equidistant distance series is found. The benefit of transforming the time series into a distance series is that it enables the comparison of splice data regardless of the belt speed, since the position of the splices and the pulley will always be the same.

4.4. Estimating the Belt Signature

Now that the measured signal is available as a distance series, it is possible to relate a specific position on the belt with a specific point in the distance series, if the starting point of the belt in the distance series is known. It is not necessary to know an exact starting point, but it should be known where a revolution of the belt starts and ends. The belt itself has a surface structure that will produce displacements at the scraper. This displacement will occur repeatedly in the distance series. However, the distance series is affected by disturbances, like e.g. the pulley surface structure, damage to the belt and operation related disturbances. Understanding the stochastic nature of the disturbances, the sinusoidal disturbance behavior of the pulley, and assuming the belt surface is smooth a Kalman filter can be employed to estimate the belt surface and its derivative $dbs(d)$. Note that the Kalman filter is not realized in the time domain but in the distance domain.

The underlying model for the Kalman filter is defined as a sinusoidal motion which is biased by the surface signature

$$\begin{aligned} x_{k+1} &= \begin{bmatrix} 1 & d_S & 1 & 0 \\ -\omega^2 d_S & 1 & 0 & 0 \\ 0 & 0 & 1 & d_S \\ 0 & 0 & 0 & 1 \end{bmatrix} x_k + \nu_k \\ z_k &= \begin{bmatrix} 1 & 0 & 0 & 0 \end{bmatrix} x_k + \eta_k \end{aligned} \tag{5}$$

where ω is the spatial frequency of the sinusoidal-like motion induced by the pulley structure, d_S is the spatial sample rate, η and ν are normally distributed noise terms, and k denotes the sample instance. Further, the state vector is defined as

$$x = \begin{bmatrix} z & \frac{\partial z}{\partial d} & bs & \frac{\partial bs}{\partial d} \end{bmatrix}^T \tag{6}$$

The Kalman filter as described by Gustafsson (2000) is implemented using (5) as the model, initial conditions $x_0 = [z_0 \; 0 \; 0 \; 0]^T$, and the variance of the sensor signal as R. Setting the covariance matrix Q reflecting ν and initial conditions for the state covariance matrix P, is usually difficult and dependent on the situation. Here, Q is chosen as a diagonal matrix $Q = diag(10^{-1}, 10^{-1}, 10^{-7}, 10^{-9})$ and the initial condition $P_0 = 100 \cdot Q$.

To identify belt rotations, the derivate $dbs(d)$ of $bs(d)$ is used in relation to a reference signature. Performing the estimation on several belt rotations enables the learning of a reference signature by deriving the median of all recorded repetitions of the signature, denoted $dbs_R(d)$. Note, the reference derivative signature $dbs_R(d)$ can have an arbitrary starting point on the belt. To identify a complete revolution of the belt in the estimated signature, an optimization problem can be solved that identifies the position of $bs_R(d)$ in the currently estimated $dbs(d)$, by minimizing the deviation between the two series. The localization and identification of the splices and other points of interest (POI's) for monitoring is then solved as a lookup. The identification of the start of a belt revolution is describe here. Define

$$L' = \underset{L}{\operatorname{argmin}} \frac{1}{N}\sum_{i=0}^{N}(dbs(i+L) - dbs_R(i))^2 \tag{7}$$

where N is the number of datapoints in dbs_R. The solution L' to (7) will be an index where the reference dbs_R is the most alike dbs and will describe where a new belt rotation is taken place. By having a knowledge of the splice locations in belt reference $dbs_R(d)$, it is now possible to also localize the splice locations in $z(d_k)$.

4.5. Splice and Pulley References

Similar to having reference distance series for the belt signature, references for the splices and the pulley can be derived. Moreover, the pulley surface structure is a dominant disturbance of high magnitude and the rotation of the pulley, and the belt are only rarely aligned. Thus, one and the same position on the belt will be affected by different disturbances due to the pulley surface structure. Nevertheless, by having a pulley reference and aligning it with the recorded distance series, it is possible to remove it by subtraction from the distance series. As a result, the distance series representing the changes in the belt surface can be recovered. The remaining signal components are then $\boldsymbol{z'}_{s,i}$ and its reference $\boldsymbol{z'}_{sR,i}$. Using these two series it is possible to quantify the change in the belt surface and as a result calculate condition indices, that quantify the change over the number of revolutions of the belt.

4.6. Condition indices

The condition of the splice or any POIs on the belt can be characterized by two main parameters, the vertical displacement of the surface and the longitudinal extend of the area of change. Since the belt is composed of laminated layers of rubber and reinforcement materials, the lamination can degrade and variations in thickness can occur. Damages can also lead to lose parts or bubbles that can be filled with material. Typical condition indices include:

$$\left|\left|\boldsymbol{z'}_{s,i} - \boldsymbol{z'}_{sR,i}\right|\right|_2 \tag{8}$$

$$\max\left(|\boldsymbol{z'}_{s,i} - \boldsymbol{z'}_{sR,i}|\right) \tag{9}$$

$$\min\left(|\boldsymbol{z'}_{s,i} - \boldsymbol{z'}_{sR,i}|\right) \tag{10}$$

These indices can be tracked over time and their change can be predicted if the change is smooth over the number of revolutions of the belt. These condition indices can then be used as actionable insights for decision making on maintenance and stop of operation.

5. Results & Discussions

This section will present the results from tests that have been conducted at an industrial site. For this end, the solution was implemented in a cloud-based architecture as depicted in Figure 2. Two HOSCH[iris] DISCOVER units were installed on two belts with lengths of approximately 550 m and the splice condition monitoring scheme was adapted to the pulleys and belt. The tests were conducted to assess the speed estimation, belt signature estimation, and the condition monitoring.

For the condition monitoring specific tests were conducted, where rubber patches were glued to the belt surface. The splice areas themselves were newly vulcanized, which means they should not be estimated to a severe condition.

5.1. Speed Estimation

The estimated speed estimates were derived from the raw data signal by the algorithm. The displacement data is shown in Figure 6a where the belt starts from a stand still. The belt speed is then increased to 30%, 50%, 70%, 80%, 90%, 100%, and back to 30% of the maximum speed (3.3 m/s).

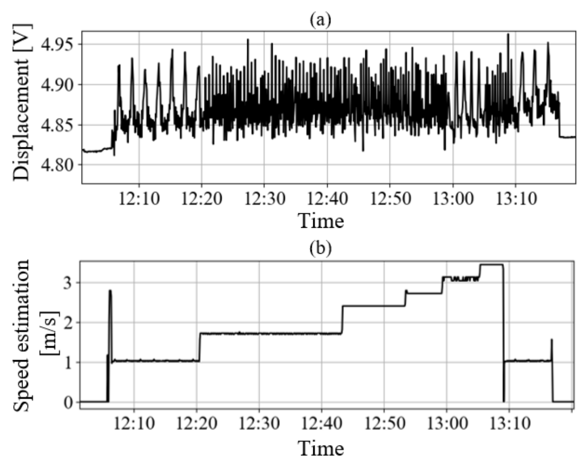

Figure 6. Speed estimation.

In Figure 6b, the estimated speed is shown. Shortly before 13:10, the speed is incorrectly estimated to be 0 m/s, which could be due to the loss of data in that time frame. There are also two spikes in the speed estimation at around 12:05 and 13:17, usually in high acceleration events when the belt is started or stopped. Using data from the control system, the speed estimation was validated rendering an error of 4% during the tests.

5.2. Belt Signature Estimation

For the belt signature estimation, no direct validation was possible, as the fine structure is estimated. Instead, the recurrence of the belt signature was used to assess the validity, by checking if the localization of the splices using the signature is correct.

In Figure **7**a, a randomly picked sequence from normal operation is shown, where the displacement data is already transformed into the distance domain using the estimated speed. The estimated derivative belt signature $dbs(d)$, with its unique features can be seen in Figure 7b. The data shows two full revolutions of the belt and the noticeable similarity of the pattern before and after 60000 cm.

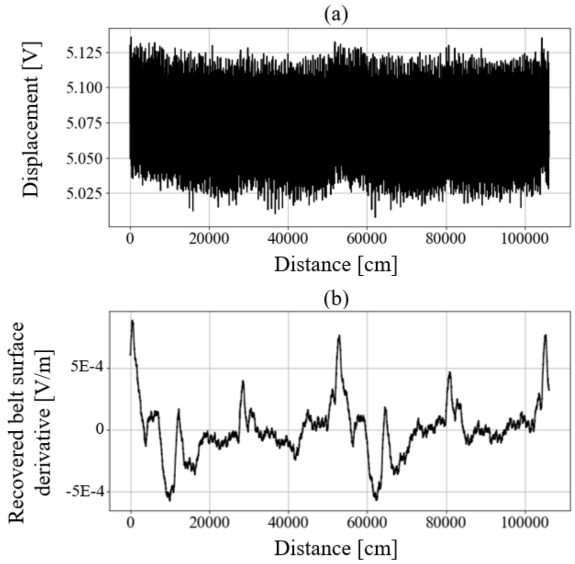

Figure 7. Transformation of displacement data to signature belt surface derivative

Using the pattern matching algorithm to align the belt rotations, the splices could be correctly localized within one meter of accuracy.

5.3. Condition monitoring of glued patches

To validate the condition assessment, artificially introduced POIs in the form of rubber patches glued to the belt surface were analyzed. For each belt, four patches of 100 x 200 x 1 mm were glued to the belt surface. The idea of the test was to track how the patches are degraded over the passages by the scraper and finally stripped from the belt surface.

To achieve this, references were created for each patch area and the already existing belt signatures and pulley references were utilized, which are generally true in the monitoring scheme. The belt conveyors were then operated as usual.

For the condition assessment of the patches the index in (9) is used and shown in Figure 8. The degradation of the patch is clearly distinguishable at about 13 belt rotations, and after about 21 rotations, it is no longer visible as it was removed from the belt by the scraper. This shows that POIs can be monitored and that changes in their behavior are estimated by in the monitoring scheme. However, the intensity of the patch degradation is not constant nor monotonically increasing each revolution and there is also some variation in the condition index.

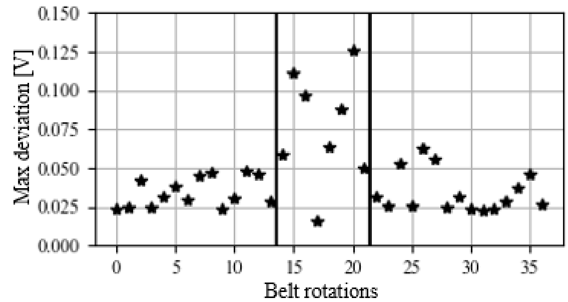

Figure 8. Maximum deviation of the belt before, while and after a patch was added.

Since the patches have sharp front edges, the collision induces an impulse on the scraper with subsequent movement. At the same time the scraper movement is sampled at a rate of 100 Hz. Depending on the alignment of the impulse with the sampling of the sensor signal and the belt speed, the maximum displacement might not be recorded, yielding a variability and error in the condition index. Nevertheless, the degradation phase of the patch is clearly captured by the scheme.

5.4. Condition monitoring of the splices

As already noted, the splices were newly vulcanized yielding a very smooth surface, which requires operation to take place over a long period of time (usually longer than a year). It was therefore expected that the splices would not generate any impact on the condition index. For the test, sequences from normal operation of the belt conveyor are used and information from inspections was collected.

Again, the maximum deviation index as given in (9) was used to assess the condition. The expectation from the test was that the index would not show any high values. In total 150 belt revolutions were assessed, which were received in batches of 10 minutes.

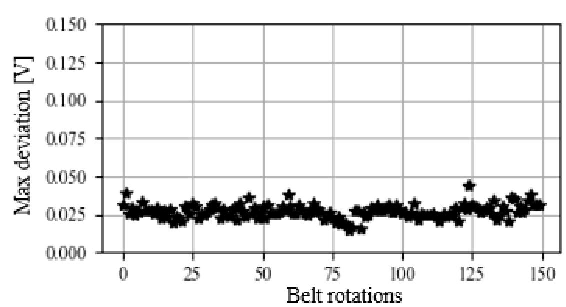

Figure 9. Maximum deviation of the belt for a splice area.

In Figure 9 it can be seen that no higher peaks are visible and that the condition index varies around a low value, which is comparable to the lower value ranges that can be seen in Figure **8**. The inspections during the normal operation also confirmed that the splices are in good condition throughout the test period. It can therefore be concluded that the monitoring scheme is not generating false indications during normal operation and replicates the condition of the splices correctly.

6. Conclusion

In this work, the fully automated condition monitoring of belt splices within operational belt conveyor systems was investigated. It is shown how the belt speed can be estimated from a signal displacement signal, how a point of interest on a conveyor belt can be localized and its degradation can be monitored. For this end, typical statistical and Bayesian filtering approaches are applied together with simple learning schemes that provide data driven models of the belt, pulleys, and normal conditions of the points of interest.

Based on the conducted tests and their assessment it can also be concluded that the condition monitoring of the belt surface using the displacement signal of a single HOSCH^{iris} DISCOVER IoT device is feasible and that actionable insights on the degradation of the belt can be provided to operators and maintenance staff to ensure safe operation. The proposed solution is now online and part of the normal operation in an industrial plant.

Future work will target the collection of experience from the solution in normal operation, the benchmarking of used methods with other approaches, and assessing the effectiveness in capturing degradation events early on and in good time for decision making on operation and maintenance.

References

Alport, M., Govinder, P., Plum, S., & Van Der Merwe, L. (2001). Identification of conveyor belt splices and damages using neural networks. *Bulk Solids Handling, 21*(6), 622-627.

Bancroft, B., Fromme, C., & Pilarski, T. (2003). Belt Vision System for Monitoring Mechanical Splices. *Proceedings of Longwall USA International Exhibition and Conference '03*.

Belt Condition Monitoring (2024). *Roxon.* Available at: https://roxon.com/hx-products/ (Accessed: 22 March 2024).

Gustafsson, F. (2000). Adaptive filtering and change detection (Vol. 1). New York: Wiley.

Harrison, A. (1985). A magnetic transducer for testing steel-cord deterioration in high-tensile strength conveyor belts. *NDT International, 18* (3), 133-138. https://doi.org/10.1016/0308-9126(85)90197-X

Kozłowski, T., Wodecki, J., Zimroz, R., Błażej, R., & Hardygóra, M. (2020). A diagnostics of conveyor belt splices. *Applied Sciences*, *10*(18), 6259. https://doi.org/https://doi.org/10.3390/app10186259

Min, H. (2010) 'Research on the Splice Breakage Monitoring System for Steel-Cord Belt Conveyor', *2010 International Conference on Measuring Technology and Mechatronics Automation*, pp. 223–226. doi:10.1109/icmtma.2010.86.

Weimann C, Kiel M (2020). Gurtabstreifer und Verfahren zum Betrieb eines Gurtabstreifers (German Patent No. DE102018123799A1)

Biographies

Henrik Lindström received his MSc. in Engineering Physics from Lund University, Sweden in 2022. He is currently working as an analytics developer at Predge AB. His work includes condition monitoring and health prediction of conveyor belts, railway turnouts and rail wagons.

Johan Öhman is an Analytics Developer at Predge AB. He holds an MSc in Engineering Physics (2015), Luleå University of Technology, and a PhD degree in Experimental Mechanics (2020), also from Luleå University of Technology. His research interests are physics-based, and data driven modeling of industrial systems.

Vanessa Meulenberg is an Analytics Developer and Project Manager at Predge AB. She completed her BSc. in Aeronautical Engineering from Inholland University of Applied Sciences and MSc. in Composite Materials at Luleå University of Technology.

Reiner Gnauert is the Head of Digital Business Development at HOSCH Fördertechnik GmbH. He holds an MSc. in Automation Control Avionics from Hamburg University of Technology. He has a long track record in conveyor belt monitoring and a history in validation and verification in the aviation industry.

Claus Weimann is the Head of Research and Development at HOSCH Fördertechnik GmbH. He holds an MSc. in Mechanical Engineering at RWTH Aachen University. He develops new products for conveyor belts at HOSCH with a focus on scraper technology.

Wolfgang Birk is the CTO at Predge AB and Professor of Automatic Control. He holds a M.Sc. degree in Electrical Engineering from University of Saarland (1997), a Ph.D. degree in Automatic Control from Luleå University of Technology (2002), and Professor of Automatic Control (2015). He has a background in the development of condition monitoring systems, process control systems for resource efficiency as well as active safety systems in the automotive sector. His research work has led to control and monitoring solutions in several industries. In the railway sector, his main interest and expertise is the use of on-board, way-side, and track monitoring systems for condition monitoring in operation and maintenance.